

Timing the millisecond pulsars in 47 Tucanae

P. C. Freire¹, F. Camilo², D. R. Lorimer³, A. G. Lyne¹, R. N. Manchester⁴
and N. D’Amico⁵

¹University of Manchester, Jodrell Bank Observatory, Macclesfield, Cheshire, SK11 9DL, UK

²Columbia Astrophysics Laboratory, Columbia University, 550 West 120th Street, New York, NY 10027, USA

³NAIC, Arecibo Observatory, HC3 Box 53995, Arecibo, PR 00612, USA

⁴Australia Telescope National Facility, CSIRO, P.O. Box 76, Epping, NSW 1710, Australia

⁵Osservatorio Astronomico di Bologna, Via Ranzani 1, 40127 Bologna, Italy

Accepted for publication by MNRAS, 2001 March 9

ABSTRACT

In the last ten years 20 millisecond pulsars have been discovered in the globular cluster 47 Tucanae. Hitherto, only three of these pulsars had published timing solutions. Here we improve upon these three and present 12 new solutions. These measurements can be used to determine a variety of physical properties of the pulsars and of the cluster. The 15 pulsars have positions determined with typical errors of only a few milliarcseconds and they are all located within $1\frac{1}{2}$ of the cluster centre. Their spatial density within that region is consistent with a distribution of the type $n(r) \propto r^{-2}$, with a sudden cutoff outside 4 core radii. Two pulsars have a projected separation of only $0''.12$, and could be part of a triple system containing two observable pulsars. We have measured the proper motions of five of the pulsars: the weighted mean of these, $\mu_\alpha = (6.6 \pm 1.9) \text{ mas yr}^{-1}$ and $\mu_\delta = (-3.4 \pm 0.6) \text{ mas yr}^{-1}$, is in agreement with the proper motion of 47 Tucanae based on *Hipparcos* satellite data. The period derivatives measured for many of the pulsars are dominated by the dynamical effects of the cluster gravitational field, and are used to constrain the surface mass density of the cluster. The pulsar accelerations inferred from the observed period derivatives are consistent with those predicted by a King model using accepted cluster parameters. We derive limits on intrinsic pulsar parameters: all the pulsars have characteristic ages greater than 170 Myr and have magnetic fields smaller than 2.4×10^9 Gauss; their average characteristic age is greater than ~ 1 Gyr. We have also measured the rate of advance of periastron for the binary pulsar J0024–7204H, $\dot{\omega} = (0.059 \pm 0.012)^\circ \text{ yr}^{-1}$, implying a total system mass $1.4^{+0.9}_{-0.8} M_\odot$ with 95% confidence.

Key words: binaries: general — globular clusters: individual (47 Tucanae) — pulsars: general

1 INTRODUCTION

Among the globular clusters in the Galactic system, 47 Tucanae (henceforth 47 Tuc) holds the record for the number of known pulsars: 20 to date (Manchester et al. 1991; Robinson et al. 1995; Camilo et al. 2000). Camilo et al. estimated the total number of potentially detectable pulsars in this cluster to be at least 200. The known pulsar population of 47 Tuc is very different from the population in the Galactic disk: all of the pulsars have periods less than 8 ms, and 13 are members of binary systems. Radio images of the cluster (Fruchter & Goss 2000; McConnell & Ables 2000) show three scintillating point sources, the positions of which coincide with the brightest known pulsars in the cluster: 47 Tuc C, D and J. It is therefore improbable that any bright pulsars remain to be discovered, even with the severe selection effects against

the detection of binaries with very short orbital periods and pulsars with very short rotational periods noted by Camilo et al. (2000).

In addition to this set of pulsars, there is a collection of other exotic objects near the core of 47 Tuc: at least 9 X-ray sources (Hasinger, Johnston & Verbunt 1994; Verbunt & Hasinger 1998) and more than 20 blue stragglers (Guhathakurta et al. 1992). Evidence has also been found for large numbers of cataclysmic variables in the core (Edmonds et al. 2001, in preparation). The high stellar density necessary for the formation of these objects may increase the rate of exchange of stars in binaries (Hut, Murphy & Verbunt 1991), leading to the formation of low-mass X-ray binaries and millisecond pulsars, a process addressed by Rasio, Pfahl & Rappaport (2000) for the specific case of 47 Tuc.

Table 1. Parameters of the globular cluster 47 Tuc.

Parameter	Value	Reference
Centre R.A., $\alpha_{47 \text{ Tuc}}$ (J2000)	$00^{\text{h}}24^{\text{m}}05^{\text{s}}29 \pm 0^{\text{s}}28$	(De Marchi et al. 1996)
Centre Decl., $\delta_{47 \text{ Tuc}}$ (J2000)	$-72^{\circ}04'52''3 \pm 1''3$	(De Marchi et al. 1996)
Distance, D	$5.0 \pm 0.4 \text{ kpc}$	(Reid 1998)
Age	$10.0 \pm 0.4 \text{ Gyr}$	(Gratton et al. 1997)
Total mass	$(1.07 \pm 0.04) \times 10^6 M_{\odot}$	(Meylan 1989)
Tidal radius	$40' (58 \text{ pc})$	(Da Costa 1979)
Core radius, θ_c (r_c)	$23''1 \pm 1''7 (0.6 \text{ pc})$	(Howell, Guhathakurta & Gilliland 2000)
Escape velocity	58 km s^{-1}	(Webbink 1985)
Central density	$\sim 1 \times 10^5 M_{\odot} \text{pc}^{-3}$	(Pryor & Meylan 1993)
Central line-of-sight velocity dispersion, $v_z(0)$	$11.6 \pm 1.4 \text{ km s}^{-1}$	(Meylan & Mayor 1986)
Proper motion in R.A., μ_{α}	$7.0 \pm 1.0 \text{ mas yr}^{-1}$	(Odenkirchen et al. 1997)
Proper motion in Decl., μ_{δ}	$-5.3 \pm 1.0 \text{ mas yr}^{-1}$	(Odenkirchen et al. 1997)

Table 1 summarises the basic parameters of 47 Tuc which we use to interpret our results. This compilation has five important updates on the information tabulated by Camilo et al. (2000). First, the position of the centre of 47 Tuc is taken to be point “D” of plate 1 of De Marchi et al. (1996). We derive the absolute position of “D” by comparing its position with that of point “G” on the same plate, whose absolute position was obtained by Guhathakurta et al. (1992). Second, recent *Hipparcos* data (Reid 1998) yields a distance to 47 Tuc of 5.0 kpc, 10% larger than previously thought (Webbink 1985). Third, according to Howell, Guhathakurta & Gilliland (2000), the core radius is double the value used previously (De Marchi et al. 1996). In addition, the stellar line-of-sight velocity dispersion at the centre (Meylan & Mayor 1986) is smaller than the previously accepted value of 13.2 km s^{-1} (Webbink 1985). The fifth update is the proper motion, obtained from *Hipparcos* data: $\mu_{\alpha} = (7.0 \pm 1.0) \text{ mas yr}^{-1}$ and $\mu_{\delta} = (-5.3 \pm 1.0) \text{ mas yr}^{-1}$ (Odenkirchen et al. 1997).

The evolutionary state of the cluster is not known precisely. It is generally presumed (e.g., Djorgovski & King 1984) that the core is in a pre-collapse phase. However, other authors (e.g., de Marchi et al. 1996) suggest that the cluster underwent core collapse in the past, reaching a core radius similar to that of M15, and that it has now re-expanded with the energy provided by the creation and hardening of stellar binary systems, an important process in globular cluster evolution (Spitzer 1987). This hypothesis was based on a determination for the angular core radius of $12''$, which indicated a dynamically evolved cluster; and it can explain the large number of exotic objects observed in the cluster. However, the more recent determination of core radius (Howell, Guhathakurta & Gilliland 2000) doubles this value, casting some doubt on that conclusion, since the re-expansion would have had to be far more vigorous. Therefore the evolutionary state of the cluster remains unclear. In § 6 we discuss the properties of the observed binary pulsars, and their relevance for the solution of this problem is addressed in § 7.

Prior to the present work, the scarcity of coherent timing solutions for the pulsars in 47 Tuc did not permit the studies that require a large sample of well-timed pulsars in a single cluster to be carried out. This has only been possible to date for the eight pulsars in M15 (Anderson 1992; Phinney 1992, 1993). These studies of M15 provide much of

the theoretical background for the present work and allow a useful comparison between M15 and 47 Tuc.

The new observations presented here bring the number of pulsars with coherent timing solutions known in 47 Tuc to 15. In § 2 we describe the observations and data reduction and analysis used to obtain the new timing solutions. We present these solutions in § 3. The new solutions lead to a wealth of astrophysical results which we discuss in the rest of the paper. In § 4 we use high-precision astrometry to investigate the pulsar distribution in 47 Tuc and the proper motion of the cluster. In § 5 we derive some constraints for the surface mass density of the cluster, and limits on the characteristic ages and magnetic fields of the pulsars. In § 6 we discuss some characteristics of the binary systems, and present the rate of advance of periastron measured for 47 Tuc H. Finally, in § 7, we summarise our results and briefly discuss the prospects for future timing observations of the pulsars in 47 Tuc.

2 OBSERVATIONS AND DATA PROCESSING

Most of the early observations of 47 Tuc were made at 660 MHz using the 64-m radio telescope at Parkes, Australia, between 1989 and 1991 (Manchester et al. 1990; Manchester et al. 1991; for a summary of all observations see Table 2). These observations led to the discovery of 10 millisecond pulsars. Further observations of 47 Tuc at 430 MHz between 1991 and 1993 (Robinson et al. 1995) resulted in the discovery of one more pulsar, B0021–72N^{*}, and phase-coherent timing solutions for 47 Tuc C and D, the two brightest isolated pulsars in the cluster. For the remaining nine pulsars then known, the paucity of detections prevented the determination of any further coherent timing solutions.

In August 1997, observations of 47 Tuc were resumed at Parkes after a four-year gap. The cluster was observed on 126 days during the following 24 months. The majority of these observations were made using the central beam of a

* Because all pulsars are detected in the same telescope beam pattern, and precise positions were not available originally, the pulsars were named B0021–72A, B, etc. Objects A, B and K were later found to be spurious, so the list of pulsars in 47 Tuc starts with B0021–72C, now referred to as J0023–7204C, or 47 Tuc C.

Table 2. Summary of 10 years of observations of 47 Tuc. N_{obs} is the number of observing days, ν_c is the central radio frequency used, $\Delta\nu$ is the total bandwidth recorded, N_{chan} is the number of frequency channels per polarization, τ is the most common integration time, t_{samp} is the sampling time, and t_{res} is the time resolution for each set of observations at the central frequency. With $\Delta\nu_{\text{chan}} \equiv \Delta\nu/N_{\text{chan}}$, the time resolution is obtained using $t_{\text{res}}^2 = t_{\text{DM}}^2 + t_{\text{samp}}^2$, where $t_{\text{DM}} = 8.3 \times (\text{DM}/\text{cm}^{-3}\text{pc}) \times (\Delta\nu_{\text{chan}}/\text{MHz}) \times (\nu_c/\text{GHz})^{-3} \mu\text{s}$.

Time span	N_{obs}	ν_c (MHz)	$\Delta\nu$ (MHz)	N_{chan}	τ (min)	t_{samp} (μs)	t_{res} (μs)
7/89–5/92	47	660	32	128	74	300	350
5/91–11/93	42	430	32	256	90/60	300	440
1/98–4/98	18	660	32	256	105	125	155
8/97–8/99	108	1374	288	96	280	125	270

multi-beam system (Lyne et al. 2000) at a central frequency of 1374 MHz ($\lambda 20$ cm) with a bandwidth of 288 MHz. Incoming signals from two orthogonal polarisations were down-converted and filtered in a $2 \times 96 \times 3$ -MHz filter bank. After summing the polarisation pairs, the resulting voltages were one-bit sampled every 125 μs and, together with accurate time referencing, stored on magnetic tapes for later analysis.

Recording the raw data in this way has two benefits. First, it allows off-line searches for new pulsars to be carried out. This strategy has been remarkably successful, essentially doubling the number of pulsars known, many of which are undetectable most of the time because of interstellar scintillation (Camilo et al. 2000). Second, for timing purposes, it allows us to refine the timing models iteratively, resulting in the ephemerides reported here.

In the timing analysis, the raw data are de-dispersed and folded according to an initial ephemeris for each pulsar. In the early stages, this ephemeris is determined from variations in the observed rotational period of the pulsar in the discovery and confirmation observations. It is important that the pulsars be detected frequently, otherwise it is impossible to count unambiguously the number of pulsar rotations between two different epochs. The 20-cm observations made after August 1997 made use of the excellent sensitivity of the Parkes multi-beam system and resulted in a large increase in the detection rate for all the previously known pulsars in 47 Tuc when compared to the earlier observations at 660 MHz. This was despite the lower flux densities at 1400 MHz.

The integrated pulse profiles obtained by folding the data at the predicted pulse period are then cross-correlated with a low-noise “standard” pulse profile (see Camilo et al. 2000 for the 20-cm profiles). This allows the determination of topocentric pulse times-of-arrival (TOAs), referred to the observatory time standard. This was related to UTC(NIST) by a radio link to the Tidbinbilla Deep Space Station and from there to NIST by a GPS common-view system. We then use the TEMPO software package[†] to calculate the corresponding barycentric TOAs using the assumed pulsar position and the JPL DE200 solar system ephemeris (<http://ssd.jpl.nasa.gov>). The differences between the measured and predicted TOAs are used to improve the parameters of the ephemeris (for further details of this process

Table 3. Timing status for the pulsars in 47 Tuc. J2000 names have not been assigned to pulsars for which there is presently no timing solution. A horizontal line separates the pulsars discovered in the early 1990s (Robinson et al. 1995) from those reported by Camilo et al. (2000). N_{TOA} is the number of TOAs used in each solution, and rms is the weighted root-mean-square of the post-fit timing residuals in μs .

Pulsar (J2000)	Orbital solution	Coherent timing solutions			
		Start MJD	Final MJD	N_{TOA}	rms
0023–7204C	isolated	48494	51406	750	19
0024–7204D	isolated	48492	51405	402	11
0024–7205E	known	48464	51406	404	22
0024–7204F	isolated	48491	51406	348	14
0024–7204G	isolated	48600	51404	72	26
0024–7204H	known	48517	51406	299	27
0024–7204I	known	50683	51406	119	27
0023–7203J	known	48491	51406	1114	7
0024–7204L	isolated	50686	51406	59	39
0023–7205M	isolated	48517	51406	80	50
0024–7204N	isolated	48515	51405	69	14
0024–7204O	known	50683	51406	210	20
47 Tuc P	known
0024–7204Q	known	50689	51405	146	29
47 Tuc R	known
47 Tuc S	known
0024–7204T	known	50683	51380	125	63
0024–7203U	known	48515	51383	178	20
47 Tuc V	not known
47 Tuc W	known

see, e.g., Taylor 1992). In the early stages, the improved ephemeris is used to reprocess the raw data. This iterative process increases the number and quality of the TOAs, which in turn are used to improve the ephemeris.

After determining the timing solutions for the 1997–1999 period, we re-analysed the raw data from the earlier observations (see Table 2). This resulted in a substantial increase in the number and quality of TOAs, especially for pulsars in binary systems, because of the much improved orbital ephemerides.

3 COHERENT TIMING SOLUTIONS FOR 15 PULSARS

The coherent timing solutions obtained from the analysis described in the previous section result in a wealth of high-precision astrometric, spin and (for the binary pulsars) orbital information. Table 3 summarises the current timing

[†] <http://pulsar.princeton.edu/tempo>

Table 4. Celestial coordinates and rotational parameters for 15 pulsars in 47 Tuc at the reference epoch of MJD 51000. In this and in the following tables, the numbers in parentheses are 1- σ confidence-level uncertainties in the last digits quoted. The positions are referred to the J2000 equinox. For all pulsars, these parameters were fitted assuming that the pulsar has the proper motion of the cluster given in Table 1 (see § 4.3). For the DMs, the error is one or less in the last digit quoted.

Pulsar	Right Ascension (^h ^m ^s)	Declination ([°] ['] ^{''})	Period (ms)	\dot{P} (10 ⁻²⁰)	DM (cm ⁻³ pc)
C	00 23 50.3511(2)	-72 04 31.486(1)	5.7567799980968(5)	-4.985(2)	24.6
D	00 24 13.8776(2)	-72 04 43.8323(9)	5.3575732850382(5)	-0.333(2)	24.7
E	00 24 11.1013(4)	-72 05 20.131(3)	3.5363291476529(7)	9.852(2)	24.2
F	00 24 03.8519(2)	-72 04 42.799(1)	2.6235793491667(3)	6.451(1)	24.4
G	00 24 07.956(1)	-72 04 39.683(7)	4.040379145748(2)	-4.215(5)	24.4
H	00 24 06.6989(7)	-72 04 06.789(3)	3.210340709441(1)	-0.162(5)	24.4
I	00 24 07.932(1)	-72 04 39.664(5)	3.484992064038(1)	-4.59(1)	24.4
J	00 23 59.4040(1)	-72 03 58.7720(9)	2.1006335458586(2)	-0.9787(4)	24.6
L	00 24 03.770(2)	-72 04 56.90(1)	4.346168005784(5)	-12.19(3)	24.4
M	00 23 54.485(3)	-72 05 30.72(1)	3.676643219590(3)	-3.832(6)	24.4
N	00 24 09.1835(9)	-72 04 28.875(7)	3.053954347392(1)	-2.186(2)	24.6
O	00 24 04.6492(5)	-72 04 53.751(3)	2.6433432956679(7)	3.032(6)	24.4
Q	00 24 16.488(1)	-72 04 25.149(7)	4.033181182805(2)	3.41(2)	24.3
T	00 24 08.541(2)	-72 04 38.91(2)	7.588479792133(9)	29.47(6)	24.4
U	00 24 09.8325(5)	-72 03 59.667(3)	4.342826691451(2)	9.524(3)	24.3

Table 5. Orbital parameters for the eight binary pulsars in 47 Tuc with known coherent timing solutions. For 47 Tuc H the value listed under T_{asc} is the time of passage through periastron.

Pulsar	P_b (days)	x (sec)	T_{asc} (MJD)	ω ([°])	e	$\dot{\omega}$ ([°] yr ⁻¹)
E	2.256844818(6)	1.981839(4)	51000.4194595(8)	218.5(7)	0.000318(4)	...
H	2.3576965(5)	2.152812(7)	51000.97359(6)	110.494(9)	0.070557(5)	0.059(12)
I	0.229792249(8)	0.038458(9)	51000.014865(8)	...	< 0.001	...
J	0.1206649386(2)	0.0404087(6)	51000.0416882(3)	...	< 0.0003	...
O	0.135974304(2)	0.045157(5)	51000.021155(2)	...	< 0.0004	...
Q	1.18908405(1)	1.462200(7)	51000.985847(2)	132(9)	0.00008(1)	...
T	1.12617678(2)	1.33847(3)	51000.317048(3)	55(6)	0.00037(4)	...
U	0.4291056829(6)	0.526953(5)	51000.0705011(6)	341(7)	0.00015(2)	...

status for the pulsars known in 47 Tuc. The orbital parameters for 47 Tuc S and T were first determined using a new technique described by Freire, Kramer & Lyne (2001), while the orbital parameters of the remaining binaries had been determined earlier (Robinson et al. 1995; Camilo et al. 2000). The timing solutions were obtained as follows.

Because the dispersion in proper motions among pulsars is expected to be very small (see § 4.3) we assume that all pulsars have the average proper motion of the cluster, whose value we take to be that determined from *Hipparcos* data (Table 1). Using TEMPO, the available 1991–1999 TOAs were fitted to a model for each pulsar containing celestial coordinates, spin parameters, and binary elements where relevant. Dispersion measures (DM) were obtained separately by measuring frequency-dependent delays across the 288-MHz bandwidth available at 1400 MHz, and the resulting values coincide with those given by Camilo et al. (2000). We also fitted astronomically meaningless time offsets between groups of TOAs obtained at different frequencies and with

different time resolution. We do this because it is difficult to make a proper absolute alignment of pulse profiles obtained at different frequencies owing to variations in pulse shapes.

In Table 4 we present the positions, rotational parameters, and DMs obtained in this way for 15 pulsars. The corresponding timing residuals for the seven isolated pulsars are displayed in Fig. 1 as a function of time.

The orbital elements for the eight binary pulsars with timing solutions are presented in Table 5, while the corresponding timing residuals are shown in Fig. 2 as a function of time, and in Fig. 3 as a function of orbital phase.

For each pulsar we list the five Keplerian parameters: binary period P_b , projected semi-major axis light travel time x , time of passage through the ascending node T_{asc} and, where measurable, longitude of periastron ω and eccentricity e . For 47 Tuc H we indicate the time of passage through periastron, rather than through ascending node, and we also list the measured rate of advance of periastron $\dot{\omega}$. For low-eccentricity binaries (all but 47 Tuc H), in which some or-

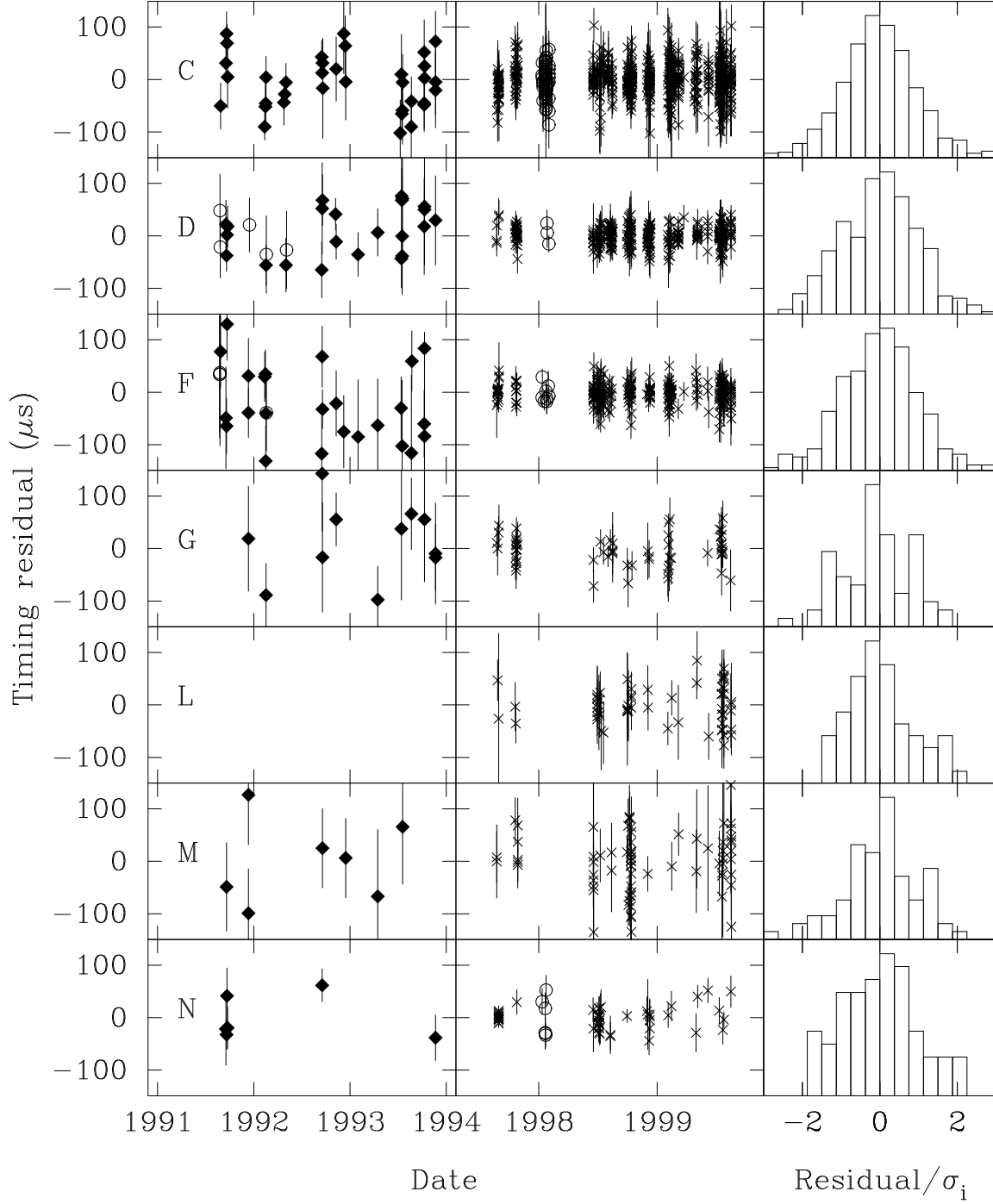


Figure 1. Post-fit timing residuals as a function of date for seven isolated pulsars. In this and in Figs. 2 and 3 the crosses, circles and filled diamonds represent residuals at 1400, 660 and 430 MHz respectively. At right we display corresponding histograms of timing residual/uncertainty for individual TOAs.

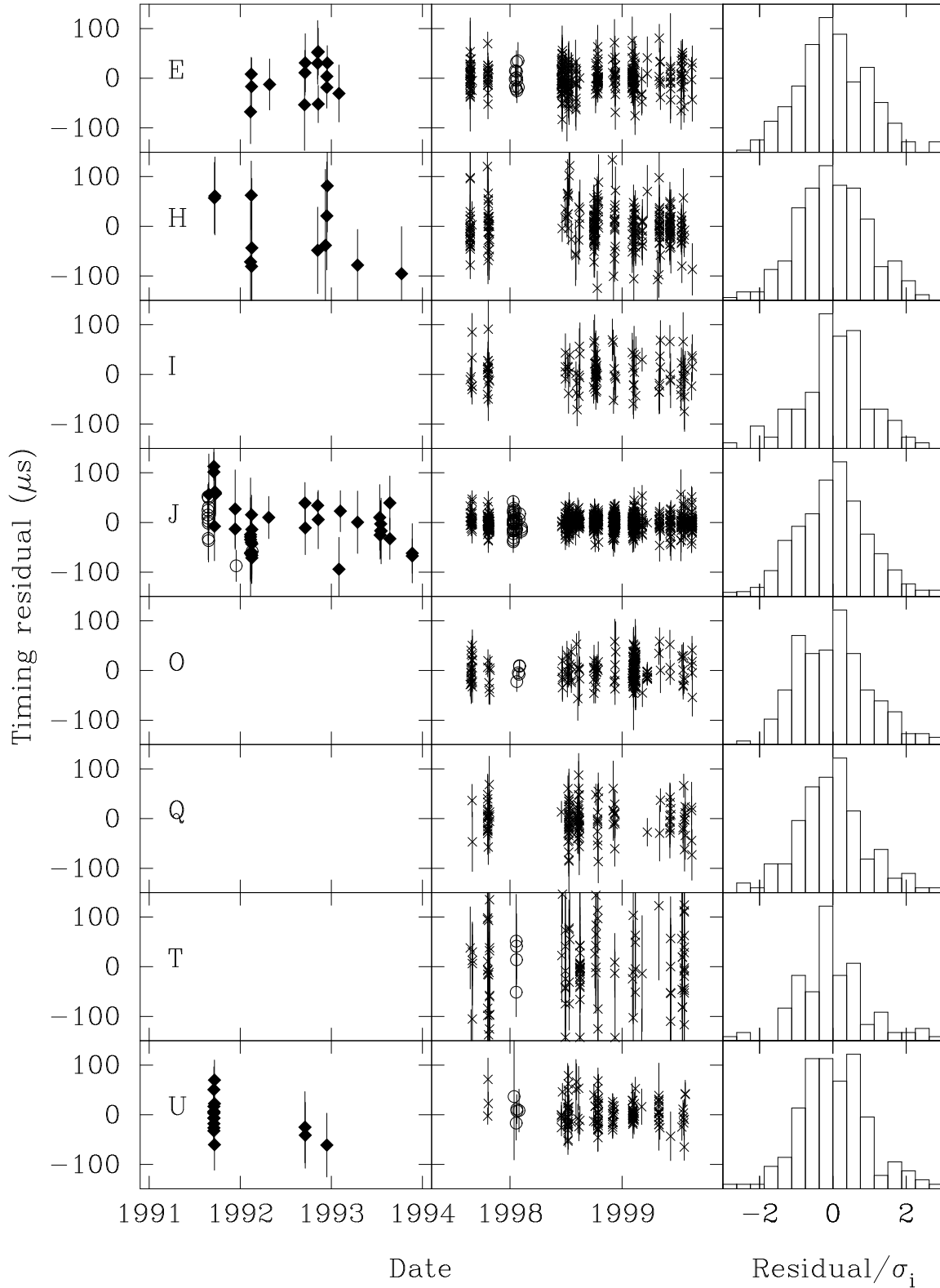


Figure 2. Post-fit timing residuals as a function of date for eight binary pulsars and corresponding histograms of timing residual/uncertainty for individual TOAs.

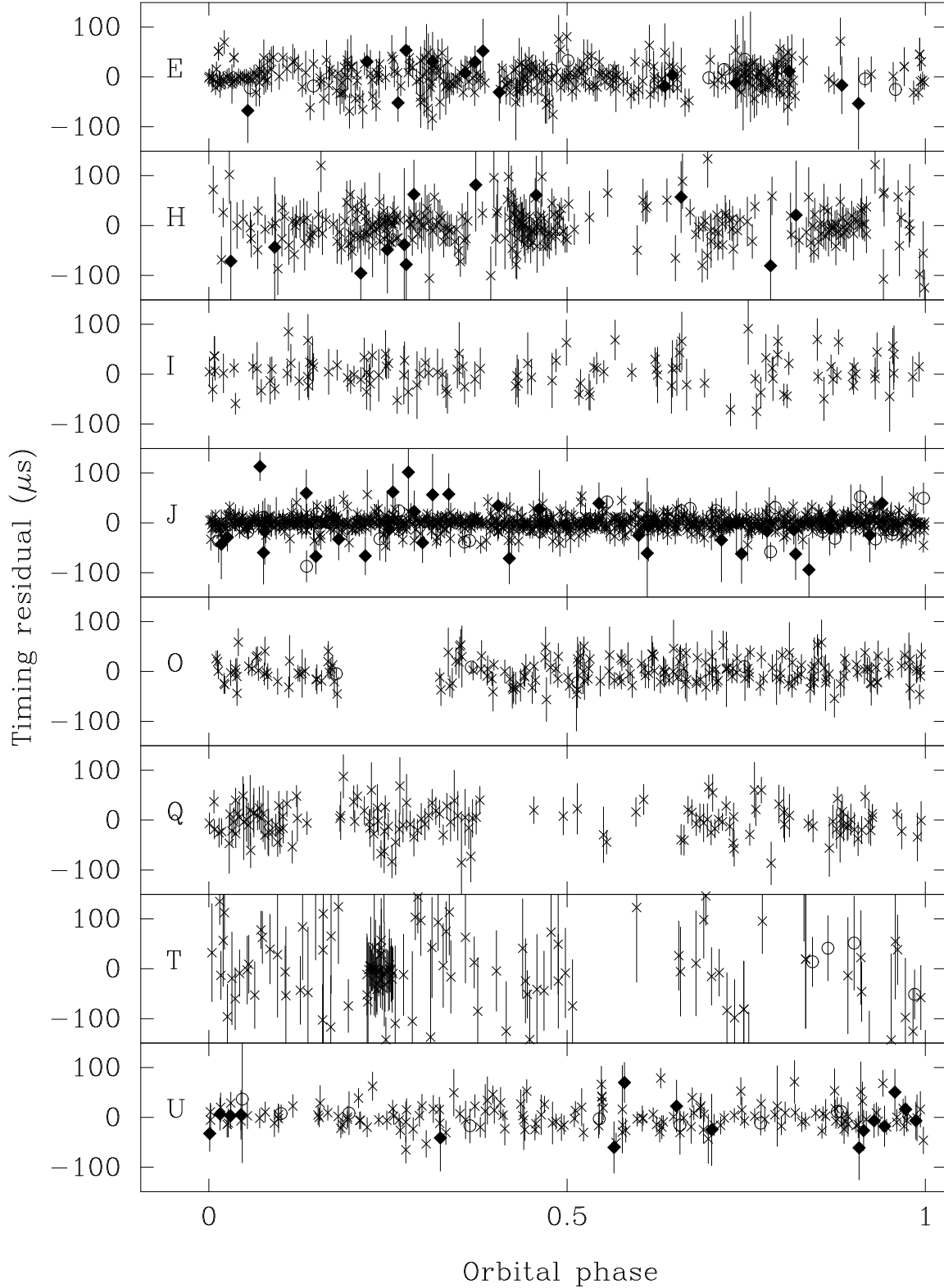


Figure 3. Post-fit timing residuals as a function of orbital phase for the eight binary pulsars whose residuals are shown as a function of date in Fig. 2. Phase is measured relative to periastron for 47 Tuc H and to ascending node for the remaining pulsars. 47 Tuc O is eclipsed for a portion of its orbit, and we do not include TOAs from this region in the timing fit.

Table 6. Proper motions of five pulsars in 47 Tuc. The average is obtained by weighting the proper motions by the inverse of each uncertainty.

Pulsar	μ_α (mas yr ⁻¹)	μ_δ (mas yr ⁻¹)
C	7.8(1.6)	-3.2(1.0)
D	7.7(1.8)	-2.6(1.6)
E	9.1(2.3)	-3.9(2.1)
F	6.6(2.6)	-3.7(2.0)
J	4.6(0.8)	-3.7(0.8)
Average:	6.6(1.9)	-3.4(0.6)

bit parameters are highly covariant in standard binary fits, we used the binary model ELL1 as implemented in TEMPO to determine the solutions presented (see Lange et al. 2001).

Finally we attempted to measure proper motions for those pulsars where we had a combination of a long time baseline and generally high-quality data. We did this with a straightforward TEMPO fit, and list the results in Table 6 for five pulsars. We also determined proper motions by comparing the positions of the pulsars in 1992–1993 and 1998–1999: for each of the two independent position measurements, no proper motion was assumed, and all TOAs used at each epoch had the same frequency (430 MHz in early 1990s, 1400 MHz in late 1990s), thus avoiding any problems with the alignment of standard profiles at different frequencies. In these fits we used the accurate rotational and binary parameters obtained previously, so only the celestial coordinates were determined. A proper motion was then calculated from the differences in position between the two epochs. These measurements are consistent with those made in the global fits, but they are less precise.

All uncertainties presented in Tables 4–6 are our best estimates of realistic 1- σ confidence levels, and in most cases are twice the formal fit uncertainties from TEMPO.

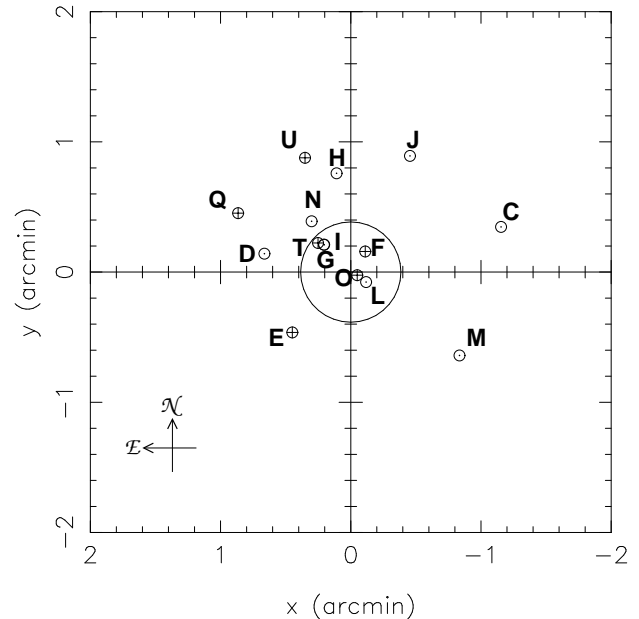
The main factors limiting the precision of the timing solutions presented in this paper are the relatively low signal-to-noise ratio of the pulsars and the low detection rate, particularly in the observations of the early 1990s. For some of the pulsars, the 20-cm flux densities are so low that they are detectable only in about 10% of all observations (see Camilo et al. 2000). Additionally, the data obtained between July 1989 and May 1991 were not used in any of the fits because the difference between the Parkes clock and UTC is not known to better than 50 μ s. This introduces significant errors that would compromise several of the measurements.

4 PULSAR POSITIONS

The timing solutions presented in the previous section bring the number of pulsars in 47 Tuc with accurately known positions to 15, and with measured proper motions to five. For easy reference, we derive from the coordinates in Table 4 the east-west (x) and north-south (y) offsets of the pulsars relative to the cluster centre. These are presented in Table 7 and depicted in Fig. 4. In the remainder of this section, we discuss the implications of these positional measurements.

Table 7. East-west (x) and north-south (y) offsets of 15 pulsars from the centre of the cluster, assumed here to be *exactly* at $\alpha = 00^{\text{h}}24^{\text{m}}05^{\text{s}}.29$ and $\delta = -72^{\circ}04'52''.3$. The errors in the offsets are 2 or less in the last digits quoted. The angular distance of each pulsar from the centre of the cluster, θ_\perp , has an accuracy limited by the uncertain absolute position of the cluster (Table 1).

Pulsar	x (arcmin)	y (arcmin)	θ_\perp (arcmin)
C	-1.1541	0.3469	1.21
D	0.6634	0.1411	0.68
E	0.4489	-0.4639	0.65
F	-0.1111	0.1583	0.19
G	0.2060	0.2103	0.29
H	0.1088	0.7585	0.77
I	0.2041	0.2106	0.29
J	-0.4547	0.8921	1.00
L	-0.1174	-0.0767	0.14
M	-0.8347	-0.6404	1.05
N	0.3008	0.3904	0.49
O	-0.0495	-0.0242	0.06
Q	0.8651	0.4525	0.98
T	0.2512	0.2232	0.34
U	0.3509	0.8772	0.94

**Figure 4.** Positions of the 15 pulsars in 47 Tuc with a timing solution plotted in the plane of the sky. The positions are given as east-west (x) and north-south (y) offsets from the centre of the cluster (see Table 7). The pulsars indicated with \oplus have positive observed period derivatives (\dot{P}), while those indicated with \ominus have negative \dot{P} . The central circle indicates the core radius.

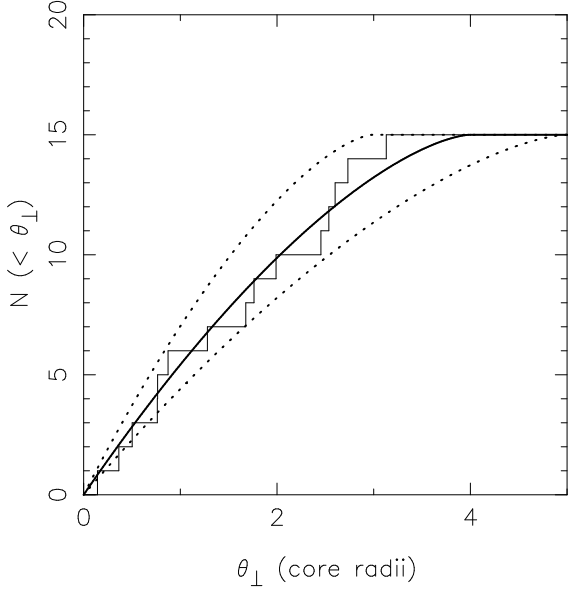


Figure 5. Cumulative radial distribution of the pulsars in 47 Tuc. This is compared with the expectation of a distribution of the type $n(r) \propto r^{-2}$ with a cutoff at 4 core radii (solid line) and 3 and 5 core radii (dotted lines).

4.1 Radial distribution

The radial distribution for the pulsars in 47 Tuc was first addressed by Rasio (2000), based on an earlier version of some of the results we present here (Freire et al. 2000). We now outline the main characteristics of this distribution and draw some conclusions from it.

The most striking characteristic of the pulsar distribution is that all the pulsars in 47 Tuc with measured positions lie within 1/2 (3 core radii) of the centre of the cluster, despite the fact that the tidal radius of 47 Tuc is about 40' (Table 1). This distribution, as we shall now see, is not an artifact introduced by the size and shape of the Parkes telescope radio beam pattern, which has a half-power radius of $\sim 7'$ at 1400 MHz.

The flux densities for most of the pulsars have been calculated by Camilo et al. (2000). Among the pulsars with a known solution, 47 Tuc N has the lowest flux density (0.03 ± 0.01 mJy). Supposing that this value is the lower limit for the flux density of a pulsar for which we can obtain a timing solution, weak pulsars like 47 Tuc U, with a flux density of 0.06 ± 0.01 mJy, are detectable in a circle with a radius of at least $7'$. There are 10 pulsars with at least this flux density, and the fact that none of these is seen outside a radius of 1/2 is therefore a true feature of the pulsar distribution, and not an artifact due to the shape of the beam. It should also be noted that the original surveys at 660 MHz (Manchester et al. 1991), with a larger telescope beam, covered an area approximately 100 times the size of the roughly arcmin-scale central region in which we now localize the 15 pulsars.

The present pulsar distribution is essentially an equilibrium distribution. The characteristic ages of these pulsars are of the order of 10^9 yr, while the relaxation time (the time it takes for a pulsar to change kinetic energy significantly through interactions with other stars) in the core of

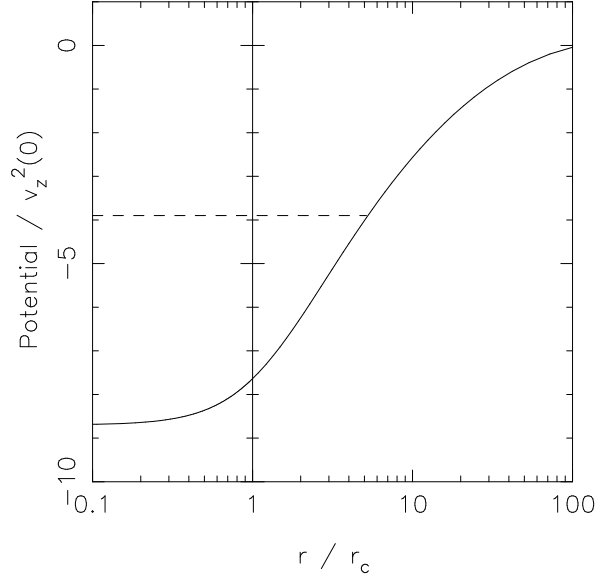


Figure 6. Globular cluster potential as a function of distance from the centre given by a King model of 47 Tuc. The maximum squared pulsar velocity at the centre is indicated by the height of the dashed line above $W(r=0) = -8.7v_z^2(0)$. The pulsars cannot travel further than about 5 core radii from the centre (see § 4.1).

47 Tuc is of the order of 10^8 yr (Djorgovski 1993). Therefore, the pulsars are expected to be in thermal equilibrium with the remaining stars, and their distribution should be merely a function of their mass and of the potential of the cluster. Indeed, the de-projected pulsar distribution is consistent with $n(r) \sim r^{-2}$ until about 4 core radii, decreasing sharply outside this radius (see Fig. 5).

This concentration of pulsars near the centre of the cluster is a consequence of mass segregation: if all objects in a cluster have reached thermal equilibrium, i.e., all stellar populations have a similar average kinetic energy, then the most massive populations, among which are the pulsars, will have smaller velocities, and therefore will dwell deeper in the potential well of the cluster. To quantify this, we note that the kinetic energy of the lighter stars in the cluster core, with mass m_{ms} , is limited by the escape velocity $v_e \equiv \sqrt{-2W(0)}$. Equating the resulting limit of kinetic energy to that of the pulsars results in a limit to the velocity of pulsars bound in the cluster core:

$$v_{p\max}^2 = (m_{ms}/m_p)v_e^2, \quad (1)$$

where m_p is the pulsar mass. As pulsars move away from the centre of the cluster under the influence of the cluster's gravitational potential their velocities decrease, eventually reaching zero at a maximum possible distance r_{lim} from the centre of the cluster.

The potential energy $U(r)$ at r_{lim} is calculated from conservation of energy:

$$U(r_{\text{lim}}) \equiv m_p W(r_{\text{lim}}) = m_p W(0) + m_p v_{p\max}^2/2, \quad (2)$$

where $W(r)$ is the cluster potential. Using equation 1 we obtain

$$W(r_{\text{lim}}) = W(0) \left(1 - \frac{m_{ms}}{m_p} \right). \quad (3)$$

This limit, with $m_{ms} = 0.8 M_{\odot}$ and $m_p = 1.45 M_{\odot}$ (the average mass for isolated and binary pulsars), is represented by a dashed line in Fig. 6, where we use a King model for the gravitational potential of 47 Tuc (King 1966; Phinney, priv. comm.). From this we derive $r_{\text{lim}} \sim 5r_c$, which is very close to the inferred $4r_c$. Therefore, the confinement of the pulsars in the inner region can be explained, to first order, as resulting from the shape of the potential and the upper limit for the kinetic energy of the pulsars. The fact that all pulsars are located close to the core is a constraint on any future more accurate model of the gravitational potential of the cluster.

Spitzer (1987) demonstrates that the distributions of two stellar species of mass m_i and m_j in thermal equilibrium with all stars in a cluster are related by

$$n_i(r) \propto n_j(r)^{m_i/m_j}. \quad (4)$$

Therefore, two stellar populations with similar masses in thermal equilibrium should have similar radial distributions. Some of the most massive blue stragglers known in 47 Tuc have masses of $1.3\text{--}1.6 M_{\odot}$ (Gilliland et al. 1998). Because this is the mass range expected for pulsars (Thorsett & Chakrabarty 1999), including binaries such as those in 47 Tuc (Camilo et al. 2000), both populations should have similar radial distributions, which is apparently the case (Rasio 2000). However we caution that the population considered by Rasio (2000) is not altogether homogeneous, having a relatively wide range of masses. Ultimately it will be useful to compare the radial distribution of just the most massive blue stragglers with that of pulsars, and in particular to determine whether they display the abrupt radial cutoff observed for pulsars.

Lastly, Spitzer shows that outside 3 core radii, the mass distribution for the dominant stellar species should be of the type $n(r) \propto r^{-2}$. Knowing this and the fact that the radial distribution of the pulsars in M15 is $n(r) \propto r^{-3.1}$ (Anderson 1992), Phinney (1992) used equation 4 to infer that the dominant stellar species near the centre of M15 is $0.9 M_{\odot}$ white dwarfs. In principle we could use the same argument to show, based on the observed pulsar distribution in 47 Tuc, that the dominant stellar species in the central region of this cluster is made of $1.3\text{--}1.6 M_{\odot}$ objects. However, the fact that the pulsars lie within (and not outside) 3 core radii may complicate this interpretation (although the ‘‘pulsar core’’ should be more compact than that of the cluster).

4.2 A triple system with two pulsars?

There is a remarkable coincidence between the celestial coordinates of 47 Tuc G, an isolated pulsar, and 47 Tuc I, a binary pulsar (see Table 7). The projected angular distance between these two pulsars is only 120 mas.

To estimate the chance probability of finding two pulsars in such close proximity, suppose that pulsars are randomly distributed in a disk of radius $18''$ (the projected angular distance of these two pulsars from the centre of the cluster). For a given pulsar, the probability of finding a second one at a projected distance of $0''.12$ or less is proportional to the area of a disk of radius $0''.12$ divided by the area of a disk of radius $18''$ or $\sim 5 \times 10^{-5}$. The probability of being at a distance larger than $0''.12$ is 0.99995. For the five pulsars known within $18''$, we have 10 different possible pairs.

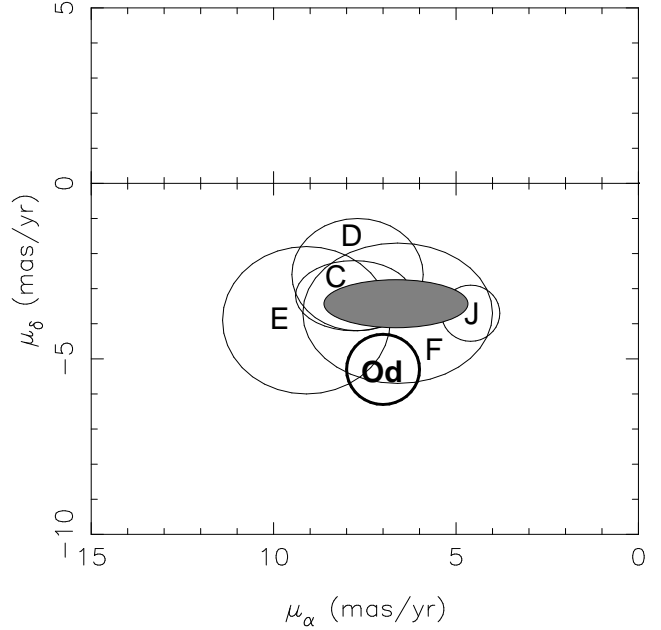


Figure 7. Measured proper motions of five pulsars in 47 Tuc. The semi-axes of the ellipses represent the $1\text{-}\sigma$ errors for the proper motions quoted in Table 6. The value for the proper motion of the cluster (Odenkirchen et al. 1997) is indicated by the thick circle. The filled ellipse indicates the motion of the cluster and its error deduced by averaging the measured pulsar proper motions.

The probability of not finding any pulsar within $0''.12$ of any other pulsar is $0.99995^{10} = 0.9995$, i.e., the overall probability of finding one or more pulsars projected within $0''.12$ of any other is 5×10^{-4} , about one in 2000.

If the pulsars are near to each other but not interacting significantly, then the acceleration caused by the cluster should be similar for both of them. In § 5 we see that their values of \dot{P}/P are similar, with a difference of $3 \times 10^{-18} \text{ s}^{-1}$, in a possible range ~ 20 times larger. Therefore, the combined probability of finding the pulsars with such close projected separation and with such similar accelerations is about one in 40,000.

Given this low formal probability of chance coincidence, it is worth considering that these two pulsars may be in a hierarchical triple system with a major axis of at least 600 a.u. A system with two components 600 a.u. apart is not likely to remain bound for long in the dense environment of a globular cluster. By considering the stellar flux with one-dimensional speeds of $v_z(r)$, an estimate for the mean time a binary system can survive in a dense environment (i.e., before it gets hit by another cluster member) is

$$\tau = (n[r]\sigma\sqrt{3}v_z[r])^{-1}. \quad (5)$$

In this expression $n(r)$ is the density of stars, $v_z(r)$ is the one-dimensional stellar velocity dispersion near the binary and σ is the cross-sectional area for the interaction of the binary with a star from the cluster. The King model for 47 Tuc predicts $n(r) \sim 4 \times 10^4 \text{ pc}^{-3}$ for this location. With $v_z(r) \sim 10 \text{ km s}^{-1}$ we estimate $\tau \sim 10^4\text{--}10^5 \text{ yr}$. This time is comparable to the orbital period of the putative binary system, and $10^{-6}\text{--}10^{-5}$ the age of the cluster. Thus, despite the

low formal probability of a chance coincidence, this simple calculation argues against the reality of such an association. Ultimately, the reality or otherwise of this system can be tested by future measurements of higher period-derivatives for the two pulsars.

4.3 Proper motions

The proper motions listed in Table 6 are displayed in Fig. 7, together with the value measured for the proper motion of the cluster by Odenkirchen et al. (1997). At the $2\text{-}\sigma$ level all these proper motions are consistent with each other.

If a pulsar is moving with a transverse velocity v_p (km s^{-1}) relative to the centre of the cluster, the difference in proper motions is $\Delta\mu = 0.21v_p/D \text{ mas yr}^{-1}$, where D is the distance to the cluster in kpc. The escape velocity of 47 Tuc is about 58 km s^{-1} (Table 1). Therefore, in order to detect a pulsar in an escape trajectory at the $3\text{-}\sigma$ level, we would have to measure relative proper motions of about 2.4 mas yr^{-1} with a precision better than 0.8 mas yr^{-1} , and we are approaching this level for 47 Tuc J (Table 6). If the pulsars are in thermal equilibrium with the surrounding stars, their relative motions are of the order of the central velocity dispersion or less, i.e., $\sim 12 \text{ km s}^{-1}$. Thus, detecting their relative motions implies measuring relative proper motions of about 0.5 mas yr^{-1} with a precision of 0.15 mas yr^{-1} . The typical precision for the positions of the weakest pulsars is around 5 mas. In order to obtain a precision of 0.15 mas yr^{-1} for these we would have to measure the positions of the pulsars again in ~ 50 years' time. However, for the brightest pulsars, with positional accuracies of about 1 mas, it will suffice to make another measurement in about 10 years, using current data-acquisition systems.

The assumption of thermal equilibrium for the pulsars implies that, with current timing precision, a measurement of the proper motions of these pulsars is in effect a measurement of the proper motion of the cluster. We can therefore make a weighted average of the five proper motions and determine the motion of the cluster, knowing that the peculiar motions of the pulsars should be smaller than the errors in the individual measurements. The weights chosen are simply the inverse of the uncertainties in each coordinate. For the currently-observed proper motions, we find the weighted average value to be $\mu_\alpha = (6.6 \pm 1.9) \text{ mas yr}^{-1}$ and $\mu_\delta = (-3.4 \pm 0.6) \text{ mas yr}^{-1}$. The uncertainties are taken to be the sum in quadrature of the weighted dispersion of the values of proper motion for the pulsars about the average, and 0.5 mas yr^{-1} , which accounts for the expected actual dispersion of proper motions.

5 PULSAR ACCELERATIONS IN THE CLUSTER POTENTIAL

Nine of the 15 pulsars in Table 4 have negative period derivatives (\dot{P}). This has been observed before for some pulsars located in globular clusters (e.g., Wolszczan et al. 1989). Rather than being due to intrinsic spin-up, negative period derivatives are thought to be caused by the acceleration of the pulsar towards the Earth in the cluster potential (see Fig. 8).

In § 5.1 we use the observed period derivatives of the

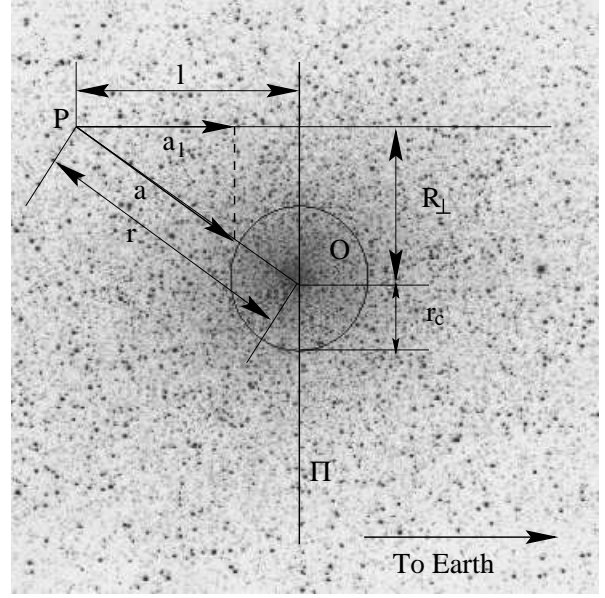


Figure 8. Geometrical parameters used in § 5: Π is a plane perpendicular to the line of sight that passes through the centre of the cluster, at point O, with core radius r_c . For a pulsar at point P, R_\perp is the projected distance to, and a is the acceleration of the pulsar towards, the centre of the cluster. The line-of-sight component of a , a_l , is the only one detectable from the Earth (located in the plane of the figure).

pulsars to estimate lower limits for the surface mass density of the cluster. We then consider the aptness of a King model together with accepted parameters for 47 Tuc in describing the accelerations experienced by the pulsars as inferred from the period derivatives (§ 5.2). We derive limits for the ages and magnetic fields of the pulsars in § 5.3.

The observed period derivative, \dot{P}_{obs} , is the sum of the pulsar's intrinsic spin-down, \dot{P}_{int} , and the effect of the acceleration along the line of sight, a_l . This sum may be negative if a negative a_l contribution is not exceeded by a positive \dot{P}_{int} ; i.e., a negative \dot{P}_{obs} implies $|a_l/c| > \dot{P}/P_{\text{int}}$. It also implies $|a_l/c| > |\dot{P}/P_{\text{obs}}|$.

The acceleration along the line of sight has several components, denoted by a_S , a_G , and a_C in

$$\left(\frac{\dot{P}}{P}\right)_{\text{obs}} = \frac{a_S}{c} + \frac{a_G}{c} + \frac{a_C}{c} + \left(\frac{\dot{P}}{P}\right)_{\text{int}}, \quad (6)$$

where the terms represent:

1. The centrifugal acceleration (Shklovskii 1970), given by

$$\frac{a_S}{c} = \frac{\mu^2 D}{c}. \quad (7)$$

This term, using the values in Table 1, amounts to $a_S/c = (+9 \pm 3) \times 10^{-19} \text{ s}^{-1}$.

2. The difference in Galactic acceleration along the line of sight between a given object and the barycentre of the solar system (a_G). This is a function of the object's Galactic latitude b , longitude l , and distance from the solar system D . For 47 Tuc we have $b = -44.9^\circ$, $l = 305.9^\circ$ and $D = 5.0 \pm 0.4 \text{ kpc}$. Using Paczynski's (1990) model of the gravitational

Table 8. Constraints on projected surface mass density for 47 Tuc obtained from nine pulsars with negative $(\dot{P}/P)_{\text{obs}}$ (see § 5.1). The distance to the cluster is taken to be 5.0 kpc.

Pulsar	$(\dot{P}/P)_{\text{obs}}$ (10^{-17} s^{-1})	R_{\perp} (pc)	$\overline{\Sigma}(< \theta_{\perp})$ ($10^3 \text{ M}_{\odot} \text{ pc}^{-2}$)	$M_{\text{cyl}}(< \theta_{\perp})$ (10^3 M_{\odot})
C	-0.91	1.75	> 18	> 170
D	-0.11	0.99	> 2.2	> 6.6
G	-1.09	0.43	> 21	> 12
H	-0.10	1.11	> 1.9	> 7.5
I	-1.36	0.43	> 27	> 15
J	-0.51	1.46	> 10	> 67
L	-2.85	0.20	> 56	> 7.3
M	-1.09	1.53	> 21	> 160
N	-0.76	0.72	> 15	> 24

potential of the Galaxy, we obtain $a_G/c = (-4.5 \pm 0.2) \times 10^{-19} \text{ s}^{-1}$.

3. Accelerations due to the gravitational field of the globular cluster and its individual stars (a_C). This is the most interesting contribution from an astrophysical point of view.

Contributions 1 and 2 total $(+5 \pm 3) \times 10^{-19} \text{ s}^{-1}$. Henceforth, $(\dot{P}/P)_{\text{obs}}$ indicates the measured value of \dot{P}/P minus these contributions, and a_l refers solely to a_C . All conclusions in this section apply only to the pulsars with known timing solutions.

5.1 Projected surface mass density of 47 Tuc

In Fig. 8 are shown some useful geometrical parameters we use in the remainder of this section. The plane Π passes through the centre of the cluster and is perpendicular to the line of sight, and the core radius is given by $r_c = D\theta_c$. A particular observed pulsar has unknown distance to the centre of the cluster, r , and to Π , l — we know only the projected distance of the pulsar to the centre of the cluster, $R_{\perp} = D\theta_{\perp}$. The acceleration along the line of sight, a_l , is the only component potentially detectable from the Earth.

We now derive constraints for the surface mass density of the cluster in its inner regions. According to Phinney (1993), the following expression is valid to within $\sim 10\%$ for all plausible cluster models, and for all θ_{\perp} :

$$\frac{a_{l\text{max}}(\theta_{\perp})}{c} \simeq 1.1 \frac{GM_{\text{cyl}}(< \theta_{\perp})}{c\pi D^2 \theta_{\perp}^2} = 5.1 \times 10^{-19} \left(\frac{\overline{\Sigma}(< \theta_{\perp})}{10^3 \text{ M}_{\odot} \text{ pc}^{-2}} \right) \text{ s}^{-1}, \quad (8)$$

where $M_{\text{cyl}}(< \theta_{\perp})$ is the mass of all the matter with a projected distance smaller than θ_{\perp} , and $\overline{\Sigma}(< \theta_{\perp})$ is the corresponding projected surface mass density. The limit on $\overline{\Sigma}$ does not depend on estimates of the distance to the cluster or core radius. The pulsars with negative observed period derivatives provide a lower bound on $a_{l\text{max}}(\theta_{\perp})$ and therefore, with equation 8, on $\overline{\Sigma}$ and M_{cyl} . These limits are presented in Table 8.

5.2 Accounting for the pulsar accelerations

We have used a King model of 47 Tuc to calculate the gravitational potential as a function of distance to the centre of the cluster, $W(r/r_c)$, divided by $v_z(0)^2$ (Fig. 6). The input for such a model is a single parameter, the logarithm of the core radius divided by the tidal radius (King 1966).

The radial derivative of $W(r/r_c)/v_z(0)^2$ yields a “normalized acceleration”, $a_n(r/r_c)$. In order to calculate accelerations A in m s^{-2} , we need two more cluster parameters: the central dispersion of line-of-sight velocities, $v_z(0)$, and the core radius, $r_c \equiv D\theta_c$. A is obtained from

$$A(r/r_c) = \frac{a_n(r/r_c)v_z^2(0)}{D\theta_c}. \quad (9)$$

To calculate the contribution to $(\dot{P}/P)_{\text{obs}}$ of the acceleration of a pulsar at a given radius we multiply $A(r/r_c)$ by l/r , so as to obtain the line-of-sight component of the acceleration. We do not, of course, know the actual distance r of each pulsar from the cluster centre, only its projection R_{\perp} . We will therefore compare the “observed acceleration” of each pulsar to the ensemble average along the relevant lines of sight calculated from the King model, taking the pulsar distribution in the cluster to have a density proportional to r^{-2} and a cut-off radius of 4 core radii (see § 4.1).

The average acceleration along each line of sight (integrated over only one hemisphere) is thus given by

$$A_a(R_{\perp}) = \frac{1}{N} \int_{l=0}^{l=\sqrt{r_{\text{lim}}^2 - R_{\perp}^2}} \frac{\lambda^{-1}}{r^2} A(r/r_c) \frac{l}{r} dl, \quad (10)$$

where λ is a normalizing constant such that λ^{-1}/r^2 is the local linear density of simulated pulsars, and N is their total number in a column along the integration path.

How do these “average” theoretical accelerations along each line of sight compare with the observed accelerations? The observed acceleration, A_o , can be obtained for each pulsar by subtracting the intrinsic \dot{P}/P from $(\dot{P}/P)_{\text{obs}}$. Unfortunately, the intrinsic period derivative is not known. We derive limits on this quantity in § 5.3, where we also find that the average characteristic age of the pulsars is greater than ~ 1 Gyr. Here we assume that each pulsar has a characteristic age of 3 Gyr and subtract the corresponding $\dot{P}/P = +0.5 \times 10^{-17} \text{ s}^{-1}$ from each observed value (listed in Table 10) to obtain an estimate for A_o . These, along with values of A_a calculated from equation 10, are presented in Table 9.

We are now in a position to compare the “observed” and average predicted accelerations. We do this for each pulsar in the last column in Table 9. This value is significantly biased for some individual pulsars by the subtraction of a fixed $\dot{P}/P = 0.5 \times 10^{-17} \text{ s}^{-1}$, our first-order attempt at accounting for the intrinsic period derivatives. However, the average of all values in the last column of the table should be approximately unity, if the modeling described above is to be consistent with the actual accelerations experienced by the pulsars — which indeed it is, despite considerable uncertainty: $|A_o/A_a(R_{\perp})| = 1.2 \pm 0.7$.

As an additional consistency check on the King model of the cluster potential we performed a Monte Carlo simulation of the pulsar population of 47 Tuc. The aim of this simulation is to see, given reasonable input assumptions, whether we can reproduce the *distribution* of $(\dot{P}/P)_{\text{obs}}$.

Table 9. Comparison of estimates of “observed” pulsar accelerations A_o with predicted average accelerations, $A_a(R_\perp)$, derived using a King model for 47 Tuc with $D = 5.0 \pm 0.4$ kpc, $v_z(0) = 11.6 \pm 1.4$ km s $^{-1}$ and $\theta_c = 23''.1$ (see § 5.2). The maximum acceleration predicted by the model for each projected pulsar offset from the centre of the cluster, used in Fig. 9, is also listed.

Pulsar	$ A_o/c $ (10^{-17} s $^{-1}$)	$ A_a(R_\perp)/c $ (10^{-17} s $^{-1}$)	$ a_{l\max}(R_\perp)/c $ (10^{-17} s $^{-1}$)	$ A_o/A_a(R_\perp) $
C	1.38	0.6 ± 0.2	1.0 ± 0.3	2.4 ± 1.0
D	0.57	1.3 ± 0.5	1.8 ± 0.7	0.4 ± 0.2
E	2.27	1.3 ± 0.5	1.9 ± 0.7	1.7 ± 0.7
F	1.95	2.1 ± 0.8	3.6 ± 1.3	0.9 ± 0.4
G	1.56	2.0 ± 0.7	3.2 ± 1.1	0.8 ± 0.3
H	0.56	1.1 ± 0.4	1.6 ± 0.6	0.5 ± 0.2
I	1.83	2.0 ± 0.7	3.2 ± 1.1	0.9 ± 0.4
J	0.98	0.8 ± 0.3	1.2 ± 0.5	1.2 ± 0.5
L	3.32	2.0 ± 0.7	3.8 ± 1.4	1.6 ± 0.7
M	1.55	0.8 ± 0.3	1.2 ± 0.4	2.0 ± 0.9
N	1.23	1.6 ± 0.6	2.4 ± 0.8	0.8 ± 0.3
O	0.63	1.4 ± 0.5	4.0 ± 1.4	0.5 ± 0.2
Q	0.33	0.9 ± 0.3	1.3 ± 0.4	0.4 ± 0.2
T	3.37	2.0 ± 0.7	3.0 ± 1.0	1.7 ± 0.7
U	1.68	0.9 ± 0.3	1.3 ± 0.5	1.9 ± 0.7

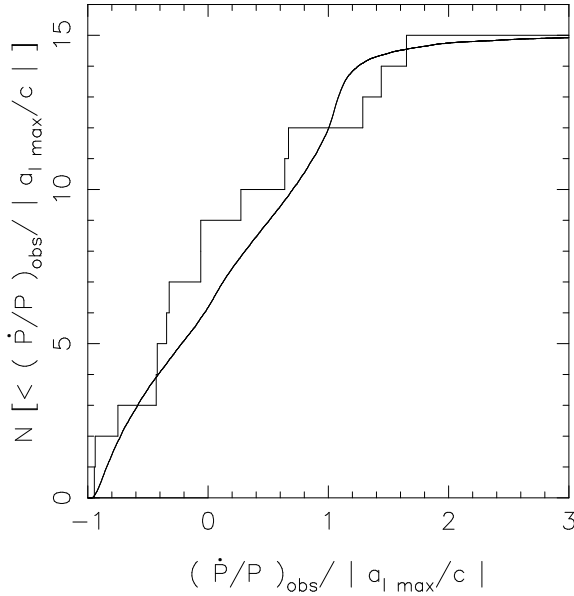


Figure 9. Cumulative distributions of $(\dot{P}/P)_{\text{obs}}/|a_{l\max}/c|$ for 15 observed pulsars, and for a simulated population (smooth curve), normalized by the observed distribution (see § 5.2).

In the simulation, we generate a spherically symmetric population of 10^6 pulsars with a radial distribution of the type $n(r) \propto r^{-2}$ and a cutoff of 4 core radii. Each of the pulsars was randomly assigned an age from a flat distribution ranging between 500 Myr and 10 Gyr — the mean $\dot{P}/P = 0.5 \times 10^{-17}$ s $^{-1}$ corresponding to what was assumed before. These assigned ages correspond to the intrinsic \dot{P}/P of each of the model pulsars. Finally, given the position of each of the model pulsars relative to the cluster centre, we calculate the contribution to \dot{P}/P from the

acceleration in the cluster determined from the King model with $D = 5.0$ kpc, $v_z(0) = 11.6$ km s $^{-1}$ and $\theta_c = 23''.1$. By adding this contribution to the intrinsic \dot{P}/P we have, for each pulsar, a model observed \dot{P}/P which can then be directly compared to the sample of 15 pulsars for which we have timing solutions.

The results of this simulation are shown in Fig. 9, where we present a cumulative plot of $(\dot{P}/P)_{\text{obs}}/|a_{l\max}(R_\perp)/c|$ for the real and simulated samples. Given the relatively small size of the observed distribution, and the straightforward simulation that we have performed, the agreement between the model and observed samples is good.

Our overall conclusion is therefore that a King model for 47 Tuc, with $D = 5.0 \pm 0.4$ kpc, $v_z(0) = 11.6 \pm 1.4$ km s $^{-1}$, $\theta_c = 23''.1$ and a small contribution from the intrinsic \dot{P}/P of the pulsars, provides a good description for the observed values of \dot{P}/P .

5.3 Limits on pulsar ages and magnetic fields

We now obtain one-sided limits for the characteristic age and the inferred surface dipole magnetic field strength of the pulsars, by calculating the maximum intrinsic period derivative for each pulsar, $\dot{P}_{\text{int max}}$. First, suppose we have a reliable estimate for the maximum possible acceleration for each pulsar’s line of sight, $a_{l\max}(R_\perp)$. Next, assume that each pulsar actually experiences such a maximum (negative) acceleration. Under such conditions, an observed $|\dot{P}/P|$ that is different from $|a_{l\max}(R_\perp)/c|$ is caused by a finite (positive) intrinsic \dot{P}/P . Hence, $(\dot{P}/P)_{\text{int}} < |a_{l\max}(R_\perp)/c| + (\dot{P}/P)_{\text{obs}}$.

After determining $\dot{P}_{\text{int max}}$ we derive a minimum characteristic age of the pulsar, $\tau_c > P/(2\dot{P}_{\text{int max}})$, and an upper limit for the magnetic field, $B < 3.2 \times 10^{19} (P\dot{P}_{\text{int max}})^{1/2}$ Gauss.

Only a reliable upper limit for the acceleration along each line of sight remains to be calculated. Phinney (1993)

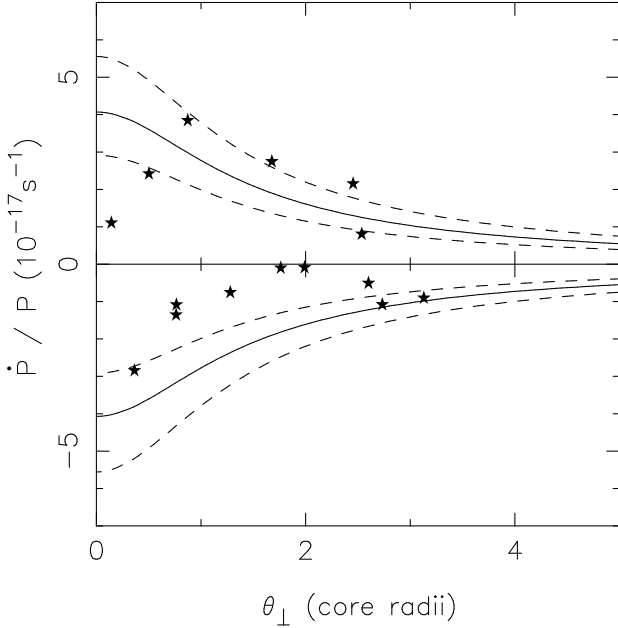


Figure 10. The values for $(\dot{P}/P)_{\text{obs}}$ (Table 10) are plotted versus θ_{\perp} for the 15 pulsars with coherent timing solutions (stars). We also plot the maximum acceleration along each line of sight calculated from a King model with the nominal distance and central velocity dispersion (solid line), and accounting for the uncertainties in those quantities (dashed lines). For all the curves and pulsar positions, we assumed θ_c to have its nominal value. See Table 1 for cluster parameters and their uncertainties.

calculated the maximum acceleration expected near the centre of a globular cluster,

$$a_{l\text{max}}(R_{\perp}) = \frac{3}{2} \frac{v_z^2(R_{\perp})}{\sqrt{r_c^2 + R_{\perp}^2}}. \quad (11)$$

This expression is valid to within $\sim 10\%$ for $R_{\perp} \lesssim 2r_c$, provided that the function $v_z(R_{\perp})$ is accurately known.

The values of \dot{P}/P observed for the pulsars (reflecting in part the gravitational potential of the cluster) do not appear to decrease greatly with R_{\perp} (Fig. 10), so we first assume conservatively that $a_{l\text{max}}(R_{\perp})$ does not decrease with R_{\perp} . Therefore, the absolute upper limit for $a_{l\text{max}}(R_{\perp})$ is $a_{l\text{max}}(0)$. Within the constraints imposed by the parameters and uncertainties in Table 1, the maximum possible value for $a_{l\text{max}}$ at the centre of the cluster is obtained with $D = 4.6$ kpc, $v_z(0) = 13.0 \text{ km s}^{-1}$ and $\theta_c = 21''.4$: according to equation 11, $a_{l\text{max}}/c = 5.74 \times 10^{-17} \text{ s}^{-1}$.

The limits for the pulsar parameters obtained with this constant maximum acceleration are presented in Table 10. All characteristic ages are larger than 170 Myr and all pulsars have magnetic fields lower than 2.4×10^9 Gauss. These values are consistent with those measured for Galactic millisecond pulsars (e.g., Camilo, Thorsett & Kulkarni 1994).

Note that these limits are extremely conservative, and are independent of any detailed modeling of the cluster. It is nevertheless clear that even with such a crudely overestimated $a_{l\text{max}}(R_{\perp})$ we can derive useful limits for the parameters of the pulsars.

By modeling the cluster and obtaining better con-

straints for $a_{l\text{max}}(R_{\perp})$, more stringent limits can be derived. For this reason, we now compare the observed pulsar \dot{P}/P with the maximum accelerations along each line of sight calculated from the King model (Fig. 10). The limits for the pulsar parameters derived from this model are also presented in Table 10. As expected, these are more constraining than those derived before. In particular, the characteristic ages for 47 Tuc C and M exceed 3 Gyr, and a simple average of the lower limits on age for all pulsars yields $\bar{\tau}_c > 0.9$ Gyr, while the magnetic field strengths of 47 Tuc J and M are less than 3×10^8 Gauss, very close to the lowest values observed among Galactic disk pulsars. These values depend, of course, on the particular cluster model used in calculating the accelerations.

Limits for the characteristic ages and magnetic fields of the pulsars in M15 have been derived by Anderson (1992), using a mass model for the cluster based on the surface luminosity density and assuming a constant mass-to-light ratio. The majority of pulsars in that cluster have characteristic ages $\sim 10^{10}$ yr (Anderson 1992), but there are signs of a relatively recent burst in pulsar formation. At least two pulsars have maximum characteristic ages $\sim 10^8$ yr and magnetic fields of about $(10\text{--}20) \times 10^9$ Gauss. This is attributed to the ongoing core collapse in M15, leading to much increased recycling of pulsars. In 47 Tuc, on the other hand, there are no visible signs of such a recent burst in pulsar formation: all the known pulsars for which a timing solution has been obtained have characteristic ages (probably much) greater than 170 Myr, weak magnetic fields, and very short rotational periods.

6 BINARY PULSAR SYSTEMS IN 47 TUC

The binary systems containing pulsars in 47 Tuc are divided into two main groups, segregated by companion mass (Camilo et al. 2000). The first is composed of binaries with very short orbital periods (1.5–5.5 hr) and companion masses $\sim 0.03 M_{\odot}$. We have timing solutions for three of these (47 Tuc I, J and O). The second group has orbital periods in the range 0.4–2.3 d and companion masses $\sim 0.2 M_{\odot}$; we refer to this group as “normal” binaries. Of these, 47 Tuc E, H, Q, T and U have a timing solution at the moment.

Coherent timing solutions give extremely detailed orbital information, and often allow the measurement of very small eccentricities. Most millisecond pulsar–white dwarf systems in the Galactic disk have very low, but measurably significant eccentricities (e.g., Camilo 1999). These are thought to result from tidal interactions between the neutron star and convective cells in the envelope of its companion during the giant phase of its evolution, and a relationship between orbital period and eccentricity can be derived for such systems (Phinney 1992). The millisecond pulsar–white dwarf systems in globular clusters often have larger eccentricities than those in the disk of the Galaxy (Phinney 1992). These are thought to result from interactions with other stars in the cluster: the denser the environment, the more likely one is to find a relatively large degree of eccentricity in the system.

The five eccentricities measured for binary pulsars in 47 Tuc (for the normal binaries 47 Tuc E, H, Q, T and U;

Table 10. Limits on period derivative, characteristic age and magnetic field for the pulsars in 47 Tuc. The $(\dot{P}/P)_{\text{obs}}$ have been corrected for the acceleration terms a_S and a_G , using $D = 4.6$ kpc. The values annotated with “2” were derived from the maximum accelerations (also indicated) calculated with an isotropic single-mass King model for 47 Tuc with the same value for the cluster distance, $v_z(0) = 13.0 \text{ km s}^{-1}$ and the nominal value for core radius (see § 5.3). The values annotated with “1” were calculated with the same parameters, except for angular core radius, where the lower limit, $\theta_c = 21''4$, was used. In this case $a_{l \text{ max}}(R_\perp)/c = a_{l \text{ max}}(0)/c = 5.74 \times 10^{-17} \text{ s}^{-1}$ (eq. 11).

Pulsar	P (ms)	$(\dot{P}/P)_{\text{obs}}$ (10^{-17} s^{-1})	$\dot{P}_{\text{int } 1}$ (10^{-19})	$\tau_{c \text{ } 1}$ (10^8 yr)	B_1 (10^9 G)	$ a_{l \text{ max}}/c $ (10^{-17} s^{-1})	$\dot{P}_{\text{int } 2}$ (10^{-19})		$\tau_{c \text{ } 2}$ (10^8 yr)		B_2 (10^9 G)	
C	5.757	−0.91	< 2.8	> 3.3	< 1.3	1.33	< 0.24	...	> 38	...	< 0.4	...
D	5.358	−0.10	< 3.0	> 2.8	< 1.3	2.48	< 1.3	...	> 6.7	...	< 0.8	...
E	3.536	2.74	< 3.0	> 1.9	< 1.0	2.60	< 1.9	> 0.05	> 3.0	< 110	< 0.8	> 0.14
F	2.624	2.42	< 2.1	> 1.9	< 0.8	4.92	< 1.9	...	> 2.2	...	< 0.7	...
G	4.040	−1.09	< 1.9	> 3.4	< 0.9	4.32	< 1.3	...	> 4.9	...	< 0.7	...
H	3.210	−0.09	< 1.8	> 2.8	< 0.8	2.21	< 0.7	...	> 7.5	...	< 0.5	...
I	3.485	−1.36	< 1.5	> 3.6	< 0.7	4.32	< 1.0	...	> 5.3	...	< 0.6	...
J	2.101	−0.51	< 1.1	> 3.0	< 0.5	1.66	< 0.24	...	> 14	...	< 0.2	...
L	4.346	−2.85	< 1.3	> 5.5	< 0.8	5.20	< 1.0	...	> 6.8	...	< 0.7	...
M	3.677	−1.08	< 1.7	> 3.4	< 0.8	1.57	< 0.18	...	> 32	...	< 0.3	...
N	3.054	−0.76	< 1.5	> 3.2	< 0.7	3.23	< 0.8	...	> 6.4	...	< 0.5	...
O	2.643	1.10	< 1.8	> 2.3	< 0.7	5.50	< 1.7	...	> 2.4	...	< 0.7	...
Q	4.033	0.80	< 2.6	> 2.4	< 1.0	1.71	< 1.0	...	> 6.3	...	< 0.7	...
T	7.588	3.84	< 7.3	> 1.7	< 2.4	4.07	< 6.0	...	> 2.0	...	< 2.2	...
U	4.343	2.15	< 3.4	> 2.0	< 1.2	1.78	< 1.7	> 0.16	> 4.0	< 42	< 0.9	> 0.3

see Table 5) are all much larger than one would expect for similar systems in the Galactic disk, and are therefore, presumably, a fossil remnant of gravitational interactions between the binary systems and other cluster stars. Rasio & Heggie (1995) calculate the expected value of this eccentricity for a system with a particular binary period that has interacted with other stars in a region of known density for a certain length of time. Unfortunately we do not know the relevant densities or interaction time scales for the pulsars observed in 47 Tuc with any degree of certainty, possibly not even to an order of magnitude. Nevertheless, taking plausible estimates for density and time scales, we derived some “predicted” eccentricities. Those for 47 Tuc E, Q, and T are within an order of magnitude of the observed values, which is as close to agreement as we can expect to attain given the uncertainties in input parameters. The computed eccentricity for 47 Tuc U is two orders of magnitude below the observed value, while that for 47 Tuc H is under-predicted by a factor of 1000.

One possible explanation for the unexpectedly large eccentricity of 47 Tuc U, and possibly that of 47 Tuc H, is that they have in the past spent a considerable amount of time in a region with a much higher stellar density than they are found in at present. For instance, if 47 Tuc L (an isolated pulsar) had spent 10^{10} yr in its present location while part of a 2.35-day binary, its computed eccentricity would be 0.15. Therefore, some of the pulsars we observe relatively far from the centre of the cluster may have non-circular orbits in the cluster potential which take them through higher-density regions periodically, or may have been ejected from higher-density regions to their present locations, leading to some of the large eccentricities measured.

Alternatively, the high eccentricity of the 47 Tuc H bi-

nary system, by far the largest in the cluster, could indicate that it obtained its present companion as an already-formed white dwarf through an exchange interaction. However, such exchanges tend to produce even higher eccentricities (Phinney 1992).

The large eccentricity of 47 Tuc H has permitted a measurement of its rate of advance of periastron: $\dot{\omega} = (0.059 \pm 0.024)^\circ \text{ yr}^{-1}$ (Table 5). Assuming that this advance is entirely due to general relativity, and not to any tidal effects (which is likely, since both stars are presumably degenerate and have negligible dimensions compared to the orbital separation), the total mass of the binary system is $1.4^{+0.9}_{-0.8} M_\odot$ (all uncertainties here are given at the $2\text{-}\sigma$ level). A mass-mass diagram is shown in Fig. 11, from which limits on the individual masses can be derived: $m_p < 2.0 M_\odot$ and $m_c > 0.1 M_\odot$. It is also improbable that $m_p < 0.4 M_\odot$ or $m_c > 0.7 M_\odot$, because this would require $\cos i > 0.95$.

7 CONCLUSIONS AND PROSPECTS

In this paper we have presented phase-coherent timing solutions for 15 millisecond pulsars in 47 Tuc. Our main conclusions can be summarised as follows.

All pulsars with known timing solutions are located less than $1/2$ from the cluster centre, and inside this region, their spatial density is of the type $n(r) \propto r^{-2}$. This distribution is different from that found in M15 ($n[r] \propto r^{-3.1}$, with no well-defined outer limit), and possibly similar to the distribution of blue stragglers in 47 Tuc with similar masses. Their confinement near the centre of the cluster is real, and not a selection effect. It is a very important constraint on any model of the potential of 47 Tuc.

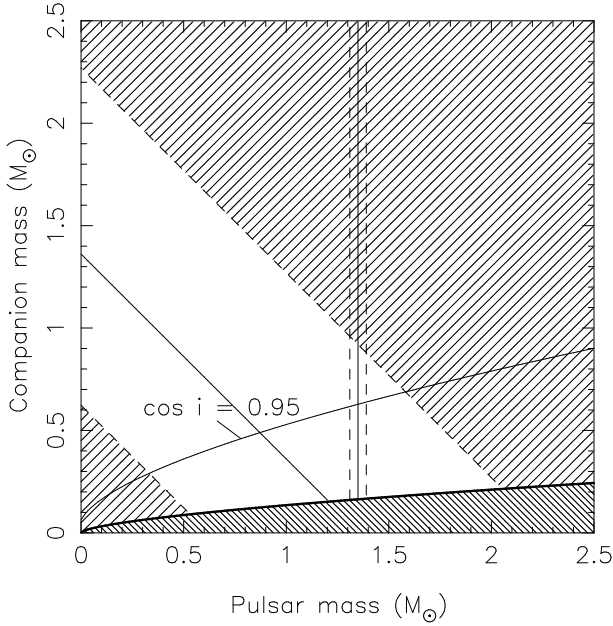


Figure 11. Mass-mass diagram for the 47 Tuc H system. The allowed range of total mass (sloping straight line surrounded by dashed lines) is derived from the measured rate of advance of periastron and its $2\text{-}\sigma$ uncertainty. The area below the thick curving line is excluded by the measured mass function and the requirement that $\cos i \geq 0$. There is a 95% a priori probability that the system lies at $\cos i \leq 0.95$. The vertical lines indicate the average measured mass for neutron stars in the radio pulsar population, $1.35 \pm 0.04 M_{\odot}$ (Thorsett & Chakrabarty 1999).

Two of the pulsars (47 Tuc G and I) have a projected separation of only 600 a.u., and similar \dot{P}/P . Although it is unlikely, they may belong to the first system known with two detectable pulsars, but further timing measurements are required to investigate this.

We have measured the proper motions of five of the pulsars in 47 Tuc. Only the general motion of the cluster is detectable, and the value calculated from averaging the proper motions of the pulsars is consistent with the proper motion of the cluster measured with *Hipparcos*.

Lower limits for the surface mass density at several radial cuts near the centre of the cluster were derived. We have also used the values of $(\dot{P}/P)_{\text{obs}}$ to obtain limits on, or estimates of, the accelerations at several projected distances from the centre of the cluster. These are consistent with a King model of the cluster using accepted values for its distance to 47 Tuc, angular core radius and central velocity dispersion.

We inferred upper limits for the magnetic fields of 15 pulsars: all are below 2.4×10^9 Gauss. Also, no pulsar has a characteristic age smaller than 170 Myr. Additionally we determined that the characteristic ages of the pulsars are, on average, greater than 1 Gyr.

The fact that none of the known binary pulsars has an orbital period larger than 2.35 days is an important result. Simulations of their formation (Rasio, Pfahl & Rappaport 2000) suggest that we should find binary pulsars with orbital periods as large as about one month. However, despite the

fact that there are no selection effects against the detection of such systems, we find none. This suggests that any binary pulsars with longer periods were either hardened by interactions with other stars, disrupted by the high stellar density near the centre of the cluster, or were simply outnumbered by tight binaries formed at a later stage. The timescale of such processes is proportional to the relaxation time, i.e. it is proportional to the time between close encounters between any two stars.

Binary formation and hardening is a source of kinetic energy for the remaining stars in the cluster and tends to delay (or in some cases reverse) core collapse (Spitzer 1987); the lack of long-period binaries therefore suggests that the core of 47 Tuc has had a density similar to or larger than the present one for a time that is much longer than the relaxation time, i.e., a few billion years (Hut 1992). If the cluster had reached the present central density in the last few hundred million years, and if it had never experienced a high-density phase before, then it should still contain binary pulsars with long orbital periods. As we have also seen, the ages of the pulsars are of the order of a few Gyr, and their large numbers in this cluster suggest that vigorous millisecond pulsar formation occurred a long time ago, which is consistent with the idea that the core of 47 Tuc was once, or has been for a long time, in a high-density state.

Another piece of evidence of possible relevance to this question comes from the higher than expected eccentricities of binaries like 47 Tuc U and H, the latter of which enabled us to measure its rate of advance of periastron, yielding a total mass $m_p + m_c = 1.4^{+0.9}_{-0.8} M_{\odot}$. These eccentricities suggest that the product of stellar density and velocity dispersion near these binaries was higher than is observed today for a long time, possibly several Gyr (§ 6). Whether this was so because the pulsars spent a considerable amount of time nearer the present-density core, or because the core was once denser, it would imply a dense core for a very long period of time.

If the core of 47 Tuc was in fact relatively dense for a few Gyr, it is likely that this contributed to the large numbers of millisecond pulsars in the cluster (via the mechanisms of binary formation and hardening in dense cores). In that case the number of millisecond pulsars in a cluster depends heavily on its previous dynamical history. This could explain why clusters with similar properties (core density, total mass, stellar mass distribution, metallicity) have large differences in their pulsar populations, in both number and kind (Kulkarni & Anderson 1996). More complete searches for pulsars in globular clusters, a better understanding of selection effects and a good determination of the evolutionary states of globular clusters will be needed to address this question.

A continuing timing programme will lead to additional and improved measurements of the proper motions of the pulsars. A measurement of the proper motions of the pulsars relative to the cluster would add constraints to the cluster mass model. Continued timing will also allow a better determination of the orbital parameters of 47 Tuc H, and will test whether 47 Tuc G and I are physically associated. Additional solutions for known pulsars may also be determined, and new pulsars will almost certainly be discovered. Continued monitoring of this cluster is therefore likely to remain a worthy enterprise.

ACKNOWLEDGEMENTS

We thank the skilled and dedicated telescope staff at Parkes for their support during this project, Vicky Kaspi, Fronez Crawford, Ingrid Stairs and Jon Bell for assistance with observations, and Chris Salter, Norbert Wex and David Nice for useful suggestions. We are also grateful to Justin Howell and colleagues for sharing their results with us prior to publication, and to Fred Rasio for very useful comments concerning the interpretation of the results. To Sterl Phinney we owe the calculation of the King model of 47 Tuc used in this paper. The Parkes Telescope is part of the Australia Telescope which is funded by the Commonwealth of Australia for operation as a National Facility managed by CSIRO. PCF gratefully acknowledges support from Fundação para a Ciência e a Tecnologia through a Praxis XXI fellowship under contract no. BD/11446/97. FC is supported by NASA grant NAG 5-9095.

REFERENCES

- Anderson S. B., 1992, PhD thesis, California Institute of Technology
- Camilo F., 1999, in Arzoumanian Z., van der Hooft F., van den Heuvel E. P. J., eds, *Pulsar Timing, General Relativity, and the Internal Structure of Neutron Stars*. North Holland, Amsterdam, p. 115
- Camilo F., Lorimer D. R., Freire P., Lyne A. G., Manchester R. N., 2000, *ApJ*, 535, 975
- Camilo F., Thorsett S. E., Kulkarni S. R., 1994, *ApJ*, 421, L15
- Da Costa G. S., 1979, *AJ*, 84, 505
- De Marchi G., Paresce F., Stratta M. G., Gilliland R. L., Bohlin R. C., 1996, *ApJ*, 468, L51
- Djorgovski S., King I. R., 1984, *ApJ*, 277, L49
- Djorgovski S. G., 1993, in Djorgovski, S. G. and Meylan, G., ed, *ASP Conf. Ser. 50: Structure and Dynamics of Globular Clusters*. Astronomical Society of the Pacific, San Francisco, p. 373
- Freire P. C., Kramer M., Lyne A. G., 2001, *MNRAS*, in press, astro-ph/0010463
- Freire P. C., Camilo F., Lorimer D. R., Lyne A. G., Manchester R. N., 2000, in Kramer M., Wex N., Wielebinski R., eds, *Pulsar Astronomy - 2000 and Beyond*, IAU Colloquium 177. Astronomical Society of the Pacific, San Francisco, p. 87
- Fruchter A. S., Goss M., 2000, *ApJ*, 536, 865
- Gilliland R. L., Bono G., Edmonds P. D., Caputo F., Cassisi S., Petro L. D., Saha A., Shara M. M., 1998, *ApJ*, 507, 818
- Gratton R. G., Fusi Pecci F., Carretta E., Clementini G., Corsi C. E., Lattanzi M., 1997, *ApJ*, 491, 749
- Guhathakurta P., Yanny B., Schneider D. P., Bahcall J. N., 1992, *AJ*, 104, 1790
- Hasinger G., Johnston H. M., Verbunt F., 1994, *A&A*, 288, 466
- Howell J. H., Guhathakurta P., Gilliland R. L., 2000, *Publ. Astr. Soc. Pac.*, 112, 1200
- Hut P., 1992, in van den Heuvel E. P. J., Rappaport S. A., eds, *X-Ray Binaries and Recycled Pulsars*. Kluwer, Dordrecht, p. 317
- Hut P., Murphy B. W., Verbunt F., 1991, *A&A*, 241, 137
- King I., 1966, *AJ*, 71, 64
- Kulkarni S. R., Anderson S. B., 1996, in Hut P., Makino J., eds, *Dynamical Evolution of Star Clusters - Confrontation of Theory and Observations*. Kluwer, Dordrecht, p. 181
- Lange C., Camilo F., Wex N., Kramer M., Backer D., Lyne A., Doroshenko O., 2001, *MNRAS*, submitted, astro-ph/0102309
- Lyne A. G. et al., 2000, *MNRAS*, 312, 698
- Manchester R. N., Lyne A. G., D'Amico N., Johnston S., Lim J., Kniffen D. A., 1990, *Nat*, 345, 598
- Manchester R. N., Lyne A. G., Robinson C., D'Amico N., Bailes M., Lim J., 1991, *Nat*, 352, 219
- McConnell D., Ables J. G., 2000, *MNRAS*, 311, 841
- Meylan G., Mayor M., 1986, *A&A*, 166, 122
- Meylan G., 1989, *A&A*, 214, 106
- Odenkirchen M., Brosche P., Geffert M., Tucholke H. J., 1997, *New Astronomy*, 2, 477
- Paczynski B., 1990, *ApJ*, 348, 485
- Phinney E. S., 1992, *Phil. Trans. Roy. Soc. A*, 341, 39
- Phinney E. S., 1993, in Djorgovski S. G., Meylan G., eds, *Structure and Dynamics of Globular Clusters*. Astronomical Society of the Pacific Conference Series, p. 141
- Pryor C., Meylan G., 1993, in *ASP Conf. Ser. 50: Structure and Dynamics of Globular Clusters*. p. 357
- Rasio F. R., Heggie D. C., 1995, *ApJ*, 445, L133
- Rasio F. A., 2000, in Kramer M., Wex N., Wielebinski R., eds, *Pulsar Astronomy - 2000 and Beyond*, IAU Colloquium 177. Astronomical Society of the Pacific, San Francisco, p. 589
- Rasio F. A., Pfahl E. D., Rappaport S., 2000, *ApJ*, 532, L47
- Reid N., 1998, *AJ*, 115, 204
- Robinson C. R., Lyne A. G., Manchester A. G., Bailes M., D'Amico N., Johnston S., 1995, *MNRAS*, 274, 547
- Shklovskii I. S., 1970, *SvA*, 13, 562
- Spitzer L., 1987, *Dynamical Evolution of Globular Clusters*. Princeton University Press, Princeton
- Taylor J. H., 1992, *Phil. Trans. Roy. Soc. A*, 341, 117
- Thorsett S. E., Chakrabarty D., 1999, *ApJ*, 512, 288
- Verbunt F., Hasinger G., 1998, *A&A*, 336, 895
- Webbink R. F., 1985, in Goodman J., Hut P., eds, *Dynamics of Star Clusters*, IAU Symposium No. 113. Reidel, Dordrecht, p. 541
- Wolszczan A., Kulkarni S. R., Middleditch J., Backer D. C., Fruchter A. S., Dewey R. J., 1989, *Nat*, 337, 531